

Solving the One-Dimensional Time-Independent Schrödinger Equation with High Accuracy: The **LagrangeMesh** Mathematica[®] Package

J.C. del Valle*

*Faculty of Mathematics, Physics, and Informatics,
University of Gdańsk, 80-308 Gdańsk, Poland*

Abstract

In order to find the spectrum associated with the one-dimensional Schrödinger equation, we discuss the Lagrange Mesh method (LMM) and its numerical implementation for bound states. After presenting a general overview of the theory behind the LMM, we introduce the **LagrangeMesh** package: the numerical implementation of the LMM in Mathematica[®]. Using few lines of code, the package enables a quick home-computer computation of the spectrum and provides a practical tool to study a large class of systems in quantum mechanics. The main properties of the package are (i) the input is basically the potential function and the interval on which is defined; and (ii) the accuracy in calculations and final results is controllable by the user. As illustration, a highly accurate spectrum of some relevant quantum systems is obtained by employing the commands that the package offers. In fact, the present work can be regarded as a user guide based on worked examples.

* juan.delvalle@ug.edu.pl

CONTENTS

I. Introduction	3
II. The one-dimensional Lagrange Mesh Method	6
A. Gauss Quadrature	6
B. Lagrange Functions	8
C. The Secular Equations and Lagrange Mesh Equations	8
III. Formulas for Lagrange Functions and Kinetic Elements	11
A. Finite Domain	11
B. Semi-Finite Domain	12
C. Infinite Domain	13
IV. Discretization, Scaling, and Mapping	13
A. Discretization of the Eigenfunctions	14
B. Scaling	14
C. Mapping	15
V. The LagrangeMesh Mathematica [®] package	16
A. Installation	16
B. Commands	17
1. BuildMesh	17
2. AvailableMeshQ	18
3. LagMeshEigenvalues	19
4. LagMeshEigenfunctions	21
5. LagMeshEigensystem	23
C. Worked Examples	23
1. Exactly Solvable Potentials	24
2. Some Non-Solvable Potentials	27
3. Possible Issues	36
VI. Conclusions	38
Acknowledgments	39
References	39

I. INTRODUCTION

Solutions to the time-independent Schrödinger equation [1] are crucial for our current understanding of quantum mechanics. However, only a handful of systems described by this equation admit exact solutions. Since the early days of quantum mechanics, the lack of exact solutions has stimulated the development of methods to find them in approximate form. In this paper, we describe and implement computationally one of such methods: the Lagrange Mesh, see [2].

In general terms, the Lagrange Mesh Method (LMM) is an approximate variational approach in which a linear combination of *Lagrange functions* approximates the exact eigenfunctions. These functions are related to a set of mesh points and the Gauss quadrature associated with this mesh. The outcome of the method is the lowest eigenvalues and eigenfunctions in approximate form.

Even though the LMM has been extensively used to study the spectrum of quantum systems¹ with few degrees of freedom (three at most), we focus on the situation when there is only one. Therefore, the main object of the present work is the one-dimensional Schrödinger equation,

$$-\frac{\hbar^2}{2m}\partial_x^2\psi(x) + V(x)\psi(x) = E\psi(x), \quad \partial_x \equiv \frac{d}{dx}, \quad (\text{I.1})$$

defined on some interval (a, b) . We assume that the potential $V(x)$ is confining and that any eigenfunction vanishes at the endpoints. For equation (I.1), we describe and implement the LMM computationally for all possible one-dimensional domains: finite, semi-finite, and infinite. Under certain conditions described in this paper, our implementation of the LMM leads to a highly accurate spectrum obtained in short CPU times.

The aim of the present paper is two-fold. From one side, we give a concrete discussion of the LMM, which can serve as a pedagogical introduction to the method itself. From the other, we introduce the **LagrangeMesh** package: a numerical implementation of the LMM written in Mathematica[®] 13. Once installed, it will provide the user with five com-

¹ See, for example, [3], [4], and [5].

mands to realize the LMM on equation (I.1). We chose this widely used programming language due to its clearness and compactness while coding, as well as for its forward compatibility with newer versions. Furthermore, we exploit the arbitrary precision arithmetic that Mathematica[®] provides specifying the option **WorkingPrecision**. In fact, the commands supplied by the **LagrangeMesh** are equipped with this option to control the loss of accuracy during calculations. It allows the user to reach and overcome benchmarks for eigenvalues and eigenfunctions in a few lines of code using a standard nowadays computer. Therefore, the package is user-friendly. Compared with previous implementations², these characteristics make the **LagrangeMesh** package superior in terms of accuracy control. It is important to mention that Mathematica[®] already counts with default commands to solve spectral problems³, particularly those of the Schrödinger type. However, they are limited to machine precision. Therefore, the **LagrangeMesh** package is unique in this aspect. On the other hand, to the best of the author’s knowledge, there is only one package in Mathematica[®] 4 devoted to solve (I.1), see [6]. It is based on a high-order Numerov scheme that requires short CPU times. However, it has some limitations: (i) long input data needed, (ii) it is mainly focused on obtaining eigenvalues; (iii) limited accuracy to machine precision. As we will show, the **LagrangeMesh** package does not have these drawbacks.

In recent years, Mathematica[®] notebooks, codes, and packages have been designed to implement different tools frequently used in quantum mechanics. Now we mention some of them. High-order corrections in perturbation theory can be calculated via the **BenderWu** package for locally one-dimensional harmonic potentials [7]. The notebook **M-CHIPR.nb** constructs potential energy functions for triatomic molecules [8]. The package **GroupMath** is oriented to Lie algebras [9]. For tight-binding calculations, we can use the **MathemaTB** package [10]. In this way, the **LagrangeMesh** will complement such tools.

The present work is organized as follows: in Sections II, III, and IV, we present a description of the LMM. The discussion is aimed to give the user the fundamental concepts behind the package. Undoubtedly, knowing the niceties and limitations of the method may lead to better performance during calculations.

In Section V, we introduce the **LagrangeMesh** package with a detailed description of

² Most of them written in FORTRAN working with double and, sometimes, quadruple precision. See [2] and references therein.

³ See built-in commands **NDEigensystem** and **NDEigenvalues**.

the usage. Actually, this Section can be regarded as a user guide based on worked examples. Specifically, we complement the discussion with concrete applications. First, we show how commands are used for obtaining the spectrum of exactly solvable potentials. These examples set the ground for the study of relevant quantum-mechanical systems/potentials: quartic anharmonic oscillator, quartic double-well with degenerate minima, shell-confined hydrogen atom, \mathcal{PT} -symmetric cubic oscillator, quasi-exactly solvable sextic anharmonic potential, and Rydberg atoms.

Those worked examples allow us to study different phenomena that appear in the quantum spectrum and glimpse the scope of the package. For instance, for the quartic double well, we can calculate the exponentially small gap between the two lowest states and study the partial sums of the semi-classical resurgent expansion [11]. In general, the results obtained by the package are shown in worked examples are compared with those found in the literature.

To simplify Section V, we present *blocks of codes* that show concrete numerical implementations. They display the input and output in the same way Mathematica[®] does. In addition, we show some plots generated in Mathematica[®] and their corresponding codes from which they were generated. We have avoided labeling the axis of plots to keep blocks as simple and compact as possible. All calculations displayed on such blocks were performed using a Mac Mini (2014) with 2.7 GHz Intel Core i5 and 8GB RAM.

II. THE ONE-DIMENSIONAL LAGRANGE MESH METHOD

Three basic ingredients are the building blocks of the LMM: the Gauss quadrature approximation, the Lagrange functions, and the secular equations. In the following Sections, we give an overview of each one. Full details can be found in [2] and references therein.

A. Gauss Quadrature

Consider the one-dimensional integral over a smooth function $f(x)$ on the interval⁴ $[a, b]$, namely,

$$\int_a^b f(x) w(x) dx, \quad (\text{II.1})$$

where $w(x) \geq 0$ is a given weight function. Frequently this integral can not be computed analytically. Nevertheless, numerical integration methods can circumvent this inconvenience. Among those methods, the Gauss quadrature approximation stands alone due to its simplicity, efficiency, and high accuracy. The basic idea of this approach is to approximate the integral (II.1) by a particular finite sum:

$$\int_a^b f(x) w(x) dx \approx \sum_{k=1}^N w_k f(x_k). \quad (\text{II.2})$$

The set $\{x_k\}_{k=1}^N$ contains the *mesh points*, while $\{w_k\}_{k=1}^N$ the (positive) *weights*. The expression shown on the right-hand side of (II.2) is the so-called *Gauss quadrature approximation*.

To determine $\{x_k\}_{k=1}^N$ and $\{w_k\}_{k=1}^N$, we demand the Gauss quadrature approximation to be exact when the function $f(x)$ is a polynomial of the degree $(2N - 1)$. As a result, it can be shown that $\{x_k\}_{k=1}^N$ and $\{w_k\}_{k=1}^N$ are real and they may be obtained by solving algebraic equations. However, there is a more efficient way to find mesh points and weights in practice. It can be demonstrated [12] that the N mesh points $\{x_k\}_{k=1}^N$ are nothing but the N zeroes of the N -degree orthogonal polynomial $\mathcal{P}_N(x)$ associated with the weight function⁵. In addition, any w_k is basically given in terms of x_k , $\mathcal{P}_{N-1}(x_k)$, and $\mathcal{P}'_N(x_k)$, see [2]. However,

⁴ The interval of integration can be finite $[a, b]$, semi-infinite $[a, \infty)$ or $(-\infty, b]$, or infinite $(-\infty, \infty)$.

⁵ For a given weight function $w(x)$, one can always construct a set of orthogonal polynomials $\{\mathcal{P}_k(x)\}_{k=1}^N$ using the Gram-Schmidt $w(x)$ process.

the well-known explicit form of the weights is irrelevant for the LMM, so we omit to present it.

Once we choose $[a, b]$ and $w(x)$, $\{x_k\}_{k=1}^N$ and $\{w_k\}_{k=1}^N$ are completely defined. For example, taking $w(x) = 1$ and the interval $[-1, 1]$, the mesh points are the N zeroes of the Legendre polynomial of order N . The name of the mesh is usually given according to the name of the polynomials involved. Therefore, in the above example $\{x_k\}_{k=1}^N$ constitutes a *Legendre* mesh of N -points.

It is worth noting that, by construction, the accuracy of the Gauss quadrature approximation (II.2) depends on how well $f(x)$ is approximated by a polynomial of degree $(2N - 1)$ in $[a, b]$. If $f(x)$ is $2N$ -times differentiable, the error estimate is given by

$$\left| \int_a^b f(x)w(x) dx - \sum_{k=1}^N w_k f(x_k) \right| \leq \frac{\int_a^b \mathcal{P}_N(x)^2 dx}{(2N)!} \sup_{\xi \in [a,b]} \{f^{(2N)}(\xi)\} , \quad (\text{II.3})$$

see [12] for details and derivation. Consequently, if the function $f(x)$ is sufficiently smooth, the accuracy of the Gauss quadrature approximation usually increases as N does. However, it may fail if $f(x)$ has singularities, discontinuities, or it is not differentiable at some points of (a, b) .

In practice, the appearance of the weight function $w(x)$ in the integrand of (II.1) can be omitted by defining an auxiliary function

$$g(x) = f(x) w(x) . \quad (\text{II.4})$$

In this way, the Gauss quadrature approximation (II.1) now takes the form

$$\int_a^b g(x) dx \approx \sum_{k=1}^N \lambda_k g(x_k) , \quad \lambda_k = \frac{w_k}{w(x_k)} , \quad k = 1, 2, \dots, N . \quad (\text{II.5})$$

Now $\{\lambda_k\}_{k=1}^N$ play the role of weights. Throughout this paper, we will work with the Gauss quadrature approximation defined according to (II.4) and (II.5). In addition, for the purposes of the present work, only meshes and weights associated with Legendre, Laguerre, and Hermite classical orthogonal polynomials are relevant.

B. Lagrange Functions

The second ingredient of the LMM is a special set of N smooth (infinitely differentiable) real functions $\{f_i(x)\}_{i=1}^N$, which are called Lagrange functions. To define them, first we need to choose a particular mesh $\{x_k\}_{k=1}^N$ and know the corresponding weights $\{\lambda_k\}_{k=1}^N$. By definition, a Lagrange function should satisfy two requirements:

1. The Lagrange condition, which is

$$f_i(x_j) = \lambda_i^{-1/2} \delta_{ij} \quad , \quad i, j = 1, 2, \dots, N \quad . \quad (\text{II.6})$$

2. Lagrange functions are orthonormal in the Gauss quadrature approximation (GQA), namely

$$\int_a^b f_i(x) f_j(x) dx \stackrel{\text{GQA}}{=} \delta_{ij} \quad . \quad (\text{II.7})$$

There are well-known prescriptions to construct Lagrange functions based on orthogonal polynomials. They can be found explicitly in [2], so we skip details. For the cases of our interest (Legendre, Laguerre, Hermite), explicit formulas of Lagrange functions are presented further down. Since the explicit form of the weights $\{w_k\}_{k=1}^N$ can be extracted from them using the Lagrange condition (II.6), we avoid presenting such expressions.

C. The Secular Equations and Lagrange Mesh Equations

The third ingredient of the LMM is the set of the so-called secular equations. These equations are useful for finding in approximate form the spectrum of a given time-independent Schrödinger equation,

$$\hat{H}\psi = E\psi \quad , \quad (\text{II.8})$$

where ψ is the wavefunction (eigenfunction), E the energy (eigenvalue), and \hat{H} the Hamiltonian.⁶ In particular, we are interested in the one-dimensional Hamiltonian of the form

$$\hat{H} = -\frac{\hbar^2}{2m}\partial_x^2 + V(x), \quad (\text{II.9})$$

where m is the mass of the particle, $V(x)$ a confining potential, and \hbar the reduced Planck constant. We assume that \hat{H} is defined in (a, b) , and the boundary conditions imposed for eigenfunctions are

$$\psi(a) = \psi(b) = 0. \quad (\text{II.10})$$

Under the above-mentioned conditions, the spectrum of the Hamiltonian (II.9) is real and discrete for the so-called *bound states*. These states are characterized by a squared-integrable eigenfunction, such that

$$\int_a^b |\psi(x)|^2 dx = 1. \quad (\text{II.11})$$

As we previously mentioned, frequently the spectral problem defined by (II.8) cannot be solved in exact form. To find an approximate solution, let us suppose that any wavefunction can be approximated by means of the linear combination

$$\psi(x) \approx \sum_{k=1}^N c_k \phi_k(x). \quad (\text{II.12})$$

Here $\{\phi_k\}_{k=1}^N$ is a set of N orthonormal functions which are chosen in such a way that boundary conditions (II.10) are fulfilled. In turn, coefficients c_k are unknown for the moment. In fact, using the variational principle, one can easily show that c_k are determined by the equations

$$\sum_{j=1}^N \left(\frac{\hbar^2}{2m} T_{ij} + V_{ij} \right) c_j = E c_i, \quad i = 1, 2, \dots, N, \quad (\text{II.13})$$

where

$$T_{ij} = -\int_a^b \phi_i(x) \partial_x^2 \phi_j(x) dx, \quad V_{ij} = -\int_a^b \phi_i(x) V(x) \phi_j(x) dx. \quad (\text{II.14})$$

⁶ The terms eigenvalue and energy will be used indistinctly, a similar situation with eigenfunction and wavefunction.

Equations (II.13) are the so-called *secular equations*, see [13] for details. They establish that, in order to find c_k , we have to diagonalize the matrix representation of the Hamiltonian constructed with the functions $\{\phi_k\}_{k=1}^N$. As a result, eigenvalues of this matrix correspond to approximations of the exact energies; meanwhile, eigenvectors contain coefficients c_k that ultimately determines the approximate wavefunctions.

Note that T_{ij} and V_{ij} in (II.14) play the usual role of kinetic and potential matrix elements, respectively. In the LMM, those matrix elements are calculated by taking $\phi_k(x)$ as Lagrange functions $f_k(x)$ and using the Gauss quadrature to compute the integrals involved in matrix elements. This approach connects the three ingredients discussed above. Under these considerations, the secular equations (II.13) now read

$$\sum_{j=1}^N \left(\frac{\hbar^2}{2m} T_{ij}^{(G)} + V_{ij}^{(G)} \right) c_j = E c_i , \quad (\text{II.15})$$

where the super-index (G) indicates that we are using the Gauss quadrature when integrating (II.14). In this sense, due to the Gauss quadrature approximation, the LMM is an approximate variational method. Equations presented in (II.15) are called *Lagrange equations*. As a consequence of using Lagrange functions and the Gauss quadrature approximation, the potential matrix elements are diagonal,

$$V_{ij}^{(G)} = V(x_i) \delta_{ij} . \quad (\text{II.16})$$

Hence, its computation is straightforward: the potential is evaluated at the mesh points. This property makes the LMM a versatile approach to study, in principle, any confining potential. The only requirement is that (II.16) approximates with high accuracy the exact potential elements shown in (II.14). On the other hand, the kinetic matrix elements $T_{ij}^{(G)}$ acquire simple and compact expressions written in terms of $\{x_i, x_j\}$ and N . Explicit formulas for relevant cases (Legendre, Laguerre, and Hermite) are presented below.

To conclude this Section, let us indicate an important remark concerning the calculation of the expectation value of a given scalar operator $\hat{O} = O(x)$. In the context of the LMM,

the expectation value of \hat{O} ,

$$\langle \hat{O} \rangle = \int_a^b \psi^*(x) O(x) \psi(x) dx , \quad (\text{II.17})$$

is calculated taking into account the Gauss quadrature approximation when integrating. Since $\psi(x)$ is a linear combination of Lagrange functions, it is easy to see that

$$\langle \hat{O} \rangle^{(G)} = \sum_{k=1}^N |c_k|^2 O(x_k) , \quad (\text{II.18})$$

where the super-index (G) indicates the usage of the Gauss quadrature. Equation (II.18) is a direct consequence of the properties (II.6) and (II.7). In summary, the calculation of expectation values of scalar operators is reduced to calculate the sum (II.18).

III. FORMULAS FOR LAGRANGE FUNCTIONS AND KINETIC ELEMENTS

Now we present three Lagrange functions defined for finite, semi-finite, and infinite intervals. They all are based on the following classical orthogonal polynomials: Legendre, Laguerre, and Hermite, respectively. For completeness, explicit formulas of the kinetic matrix elements in the Gauss quadrature approximation $T_{ij}^{(G)}$ are shown. As we will see, they are written in compact expressions. Details concerning their derivation can be found in [2] and references therein.

A. Finite Domain

For the finite interval $[-1, 1]$, it is natural to use a Legendre mesh. The corresponding Lagrange functions read

$$f_i(x) = \frac{(-1)^{N+i+1}(x+1)(1-x)}{\sqrt{2(x_i+1)(1-x_i)}} \frac{P_N(x)}{x-x_i} , \quad i = 1, 2, \dots, N . \quad (\text{III.1})$$

Here $P_N(x)$ denotes the N -th Legendre polynomial. By construction, any Lagrange function $f_i(x)$ satisfies $f_i(-1) = f_i(1) = 0$. Thus, boundary condition (II.10) is fulfilled for $a = -1$

and $b = 1$. The kinetic matrix elements $T_{ij}^{(G)}$ are given by

$$T_{i \neq j}^{(G)} = \frac{(-1)^{i+j+1}(x_i x_j + 1)}{(x_i - x_j)^2 \sqrt{(1 - x_i^2)(1 - x_j^2)}}, \quad T_{ii}^{(G)} = \frac{N(N+1)(1 - x_i^2) + 4}{3(1 - x_i^2)^2}. \quad (\text{III.2})$$

Functions shown in (III.1) are building blocks to consider arbitrary but finite, intervals of the form $[a, b]$. This can be achieved via a monotonic mapping $t : [-1, 1] \rightarrow [a, b]$, see below for discussion.

B. Semi-Finite Domain

Now we consider $[0, \infty)$. In this case, the natural mesh is a Laguerre one. The corresponding Lagrange functions are

$$f_i(x) = (-1)^{N+i} \frac{x}{\sqrt{x_i}} \frac{L_N(x)}{x - x_i} e^{-x/2}, \quad i = 1, 2, \dots, N. \quad (\text{III.3})$$

Here $L_N(x)$ denotes the N -th Laguerre polynomial. From (III.3), it is clear that any Lagrange function $f_i(x)$ satisfies $f_i(0) = f_i(\infty) = 0$. Therefore, boundary condition (II.10) is fulfilled for $a = 0$ and $b = \infty$. Explicit formulas for kinetic matrix elements $T_{ij}^{(G)}$ are

$$T_{i \neq j}^{(G)} = \frac{(-1)^{i-j}(x_i + x_j)}{\sqrt{x_i x_j}(x_i - x_j)^2}, \quad T_{ii}^{(G)} = \frac{(4N+2)x_i - x_i^2 + 4}{12x_i^2}. \quad (\text{III.4})$$

Note that with a global translation of mesh points and Lagrange functions (III.3), we can tackle domains of the form $[a, \infty)$.

Another important remark concerning functions (III.3) must be emphasized. For now, consider the reduced three-dimensional radial Schrödinger Hamiltonian

$$\hat{H} = -\frac{\hbar^2}{2m} \partial_r^2 + \frac{\hbar^2 \ell(\ell+1)}{2mr^2} + V(r), \quad 0 \leq r < \infty, \quad \ell = 0, 1, \dots \quad (\text{III.5})$$

where r denotes the radial variable in the standard spherical coordinate system, and ℓ the angular momentum quantum number. If the radial potential $V(r)$ is confining, the boundary

conditions

$$\psi(0) = 0, \quad \psi(\infty) = 0 \quad (\text{III.6})$$

are usually imposed when solving the reduced radial Schrödinger equation $\hat{H}\psi(r) = E\psi(r)$. Hence, Lagrange functions (III.3) are adequate to approximate three-dimensional radial eigenfunctions in the form of (II.12). A similar situation occurs with Lagrange functions based on Legendre polynomials (III.1): they are useful to study radial potentials when the particle is confined to a spherical core-shell or shell type cavity. Explicit examples will be presented further in the text.

C. Infinite Domain

For the one-dimensional case in $(-\infty, \infty)$, it is natural to consider the Hermite mesh. The corresponding Lagrange functions, read

$$f_i(x) = \frac{(-1)^{N-i}}{(2h_N)^{1/2}} \frac{H_N(x)}{x - x_i} e^{-x^2/2}, \quad h_N = 2^N N! \sqrt{\pi}, \quad i = 1, 2, \dots, N, \quad (\text{III.7})$$

where $H_N(x)$ denotes the N -th Hermite polynomial. It is clear that any $f_i(x)$ satisfies $f_i(-\infty) = f_i(\infty) = 0$, since it decays exponentially at large $|x|$. Therefore, boundary condition (II.10) is fulfilled for $a = -\infty$ and $b = \infty$. Kinetic matrix elements $T_{ij}^{(G)}$ are

$$T_{i \neq j}^{(G)} = (-1)^{i-j} \frac{2}{(x_i - x_j)^2}, \quad T_{ii}^{(G)} = \frac{1}{3}(2N + 1 - x_i^2). \quad (\text{III.8})$$

IV. DISCRETIZATION, SCALING, AND MAPPING

Before introducing the **LagrangeMesh** package, there are some aspects of the method that have to be discussed. In particular, they play an essential role when performing a highly accurate calculation of the spectrum.

A. Discretization of the Eigenfunctions

In the framework of the LMM, the approximate wavefunction has the representation

$$\psi(x) = \sum_{k=1}^N c_k f_k(x) , \quad a \leq x \leq b , \quad (\text{IV.1})$$

where $f_k(x)$ is the k -th Lagrange function. Note that if N is large, the number of arithmetic operations involved when evaluating (IV.1) numerically at some arbitrary point x can be huge. Therefore, the accumulation of error can play an important role and it might lead to wrong results for $\psi(x)$. There is a way to avoid such situation, but we have to abandon the idea of constructing a continuous wavefunction like (IV.1). Through the Lagrange condition (II.6), a N -point discrete version of $\psi(x)$ defined at the non-uniform mesh points $\{x_k\}_{k=1}^N$ can be obtained by noting that

$$\psi(x_k) = \frac{c_k}{\lambda_k^{1/2}} , \quad k = 1, 2, \dots, N . \quad (\text{IV.2})$$

This discrete representation usually leads to better approximations of $\psi(x_k)$ than evaluating directly via (IV.1).

B. Scaling

Higher accuracy in results predicted by the LMM can be obtained if the mesh points lie inside the region where the wavefunction is not too small. A global scaling of the mesh points in the form

$$x_k \rightarrow h x_k , \quad h > 0 , \quad k = 1, 2, \dots, N , \quad (\text{IV.3})$$

may move them to such region. We have denoted the global scaling parameter by h . If it is chosen appropriately, it can increase accuracy and improve the performance of the LMM reducing CPU times. In addition, Lagrange functions should be modified accordingly,

$$f_i(x) \rightarrow \frac{1}{h^{1/2}} f_i(x/h) . \quad (\text{IV.4})$$

The factor $h^{1/2}$ is introduced to fulfill the Lagrange condition (II.6). The usage of h not only modifies the mesh points and the Lagrange functions, it also affects the Lagrange equations. They now read

$$\sum_{j=1}^N \left(\frac{\hbar^2}{2mh^2} T_{ij}^{(G)} + V(hx_i) \delta_{ij} \right) c_j = E c_i . \quad (\text{IV.5})$$

Sometimes h can be used as a variational parameter, especially if N is large. However, the Gauss quadrature approximation used in (IV.5) may lead to a fake minimum in energy with respect to h .

C. Mapping

The above-mentioned global scaling transformation of a mesh is one of the simplest mappings that can be implemented to move the mesh points. Let us focus on the Legendre mesh and the corresponding Lagrange functions. This mesh is originally defined in $[-1, 1]$ by construction, but it can be easily mapped into $[a, b]$ using the following linear function [14],

$$t(x) = \frac{b-a}{2}x + \frac{a+b}{2}, \quad t(-1) = a, \quad t(1) = b. \quad (\text{IV.6})$$

This simple function allows us to scale, translate, reflect, and map the mesh points. In this way, we can realize the LMM in an arbitrary finite domain apart from $[-1, 1]$. Lagrange functions are modified as well according to

$$f_i(x) \rightarrow \sqrt{\frac{2}{b-a}} f_i(t^{-1}(x)) . \quad (\text{IV.7})$$

Similar considerations can be made for the Laguerre mesh. Instead of providing further details, which can be found in [2], we point out that all necessary transformations are implemented in the **LagrangeMesh** package internally and automatically. In this way, the user can study spectral problems defined in any one-dimensional interval: $[a, b]$, $[a, \infty)$, $(-\infty, b)$, and $(-\infty, \infty)$.

V. THE **LAGRANGEMESH** MATHEMATICA[®] PACKAGE

The **LagrangeMesh** package⁷ implements the LMM for solving the one-dimensional Schrödinger equation in different domains for an arbitrary potential.

While presenting the main characteristics of the package, we focus on working out particular examples to show the usage. As we mentioned previously, we use blocks of codes that display input/output to show the usage of each command. All worked examples can be found in the supplemental file called **Examples.nb**. The reader without previous experience with the LMM is encouraged to refer to it. Throughout rest of this text, the value of the reduced Planck constant \hbar is set to the unity ($\hbar = 1$).

A. Installation

The file called **LagrangeMesh.wl** contains the package. Once downloaded, there are two ways to use it, let us describe both options.

1. Full installation of the package. This can be achieved via the Install option located at the menu of Mathematica[®]: File→Install. The procedure is straightforward, so we omit details that can be found in [15]. Once the installation was successful, the package is loaded evaluating **Needs["LagrangeMesh`"]** in the notebook we want to use. Each time the kernel is restarted, we need to load the package as indicated.
2. Loading the package temporarily. This is a simple alternative that not requires installation. This option only works if the package and the notebook (in which we will perform calculations) are contained in same directory. Loading the package is achieved by evaluating **<<"path/LagrangeMesh.wl"** in the notebook file we want to work with. The explicit form of **path** is found evaluating **NotebookDirectory[]**. Each time the kernel is restarted, we need to load the package as indicated.

⁷ Designed in Mathematica[®] 13, and tested in versions 12 and 13.

B. Commands

Once installed or loaded, the **LagrangeMesh** package will provide the user five new commands. Two related to the construction of meshes and weights: **BuildMesh** and **AvailableMeshQ**; and three additional for realizing the LMM: **LagMeshEigenvalues**, **LagMeshEigenfunctions**, and **LagMeshEigensystem**. These commands are designed with the standard Mathematica[®] style (coloring, syntax, etc.). In addition, each command counts with several alert messages that can guide the user on how to correct syntax errors. Below, we describe the general use and syntax of each command.

1. BuildMesh

This command constructs mesh points (zeroes) and weights for a given type of classical orthogonal polynomial. The syntax of this command is the following:

BuildMesh[Type, Dimension, Options]

- **Type** specifies the classical polynomial, it can only take the value of the following strings "**Legendre**", "**Laguerre**", or "**Hermite**".
- **Dimension** defines the number of mesh points. Therefore, its value must be a positive integer number.
- There are two **Options** that can be specified for the command **BuildMesh**. They allow the user to compute of the Gaussian weights and to control the accuracy of calculations. Each option is described in Table I

In `In[1]`, we show how to calculate a Laguerre mesh of $N = 50$ points together with the corresponding weights using 100-digits arithmetic.

```
In[1]:= BuildMesh["Laguerre", 50, Weights→True, WorkingPrecision→100]
Out[1]:= Laguerre_50_WP_100.dat
         Laguerre_50_WP_100.Weights.dat
```

Table I: Options for the command **BuildMesh**.

Option	Description	Default Value
Weights	If the value is set to True , the weights associated to the mesh will be calculated.	False
WorkingPrecision	It specifies how many digits of precision should be maintained in internal computations. Thus, it controls the accuracy of mesh points and weights.	MachinePrecision

As output, shown in `Out[1]`, the program prints on screen the name of two files that were generated and stored. They contain the mesh points and weights, respectively. The parameters that characterize the calculation are specified in the name given. Once created, files will be automatically stored in specific directories, so they can be used in future calculations without calculating them again. The location of those files is shown in the tree diagram in Fig. 1. Using the command **BuildMesh** once, sub-directories inside **Meshes** will be automatically created.

2. **AvailableMeshQ**

Once several meshes are constructed and stored, we can generate an ordered table that shows them on screen. The latter is the primary purpose of the command. The secondary is to check if a specif mesh exists: it delivers on screen **True** in the case it does, and **False** otherwise. The syntax for this command is the following:

AvailableMeshQ[Type, Options]

- **Type** specifies the classical polynomial, it can only take the value of the following strings "**Legendre**", "**Laguerre**", or "**Hermite**".
- There are three **Options** that can be specified for the command **AvailableMeshQ**. They control the output printed on screen. Each option is described in Table II.

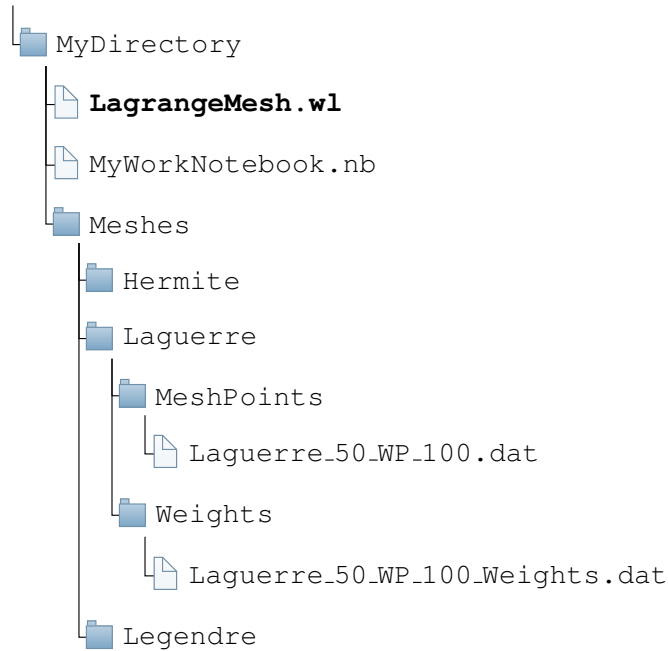


Figure 1: Tree diagram that shows the location of the stored mesh points and weights. The presence of the file **LagrangeMesh.wl** at the level of **MyWorkNotebook.nb** is optional, it is only required if we are loading the package temporarily, see text. Otherwise, it can be removed from **MyDirectory**. All directories inside **MyDirectory** will be automatically created on the first use of the command **BuildMesh**.

As an example, below we present a typical block of code with output **Out[2]** generated by the command **AvailableMeshQ**. It consists of all meshes stored with **Dimension**→**20**.

```

In[2]:= AvailableMeshQ["Laguerre", Dimension→20]
Out[2]:=

```

Dimension	WorkingPrecision	Weights
20	10	No
20	20	Yes
20	50	No
20	100	Yes
20	200	Yes
20	300	Yes
20	MachinePrecision	No

3. LagMeshEigenvalues

This command calculates the desired number of eigenvalues of the Schrödinger equation (II.8) defined in (a, b) for a given potential function $V(x)$. For a given domain, if the

Table II: Options for the command **AvailableMeshQ**.

Option	Description	Default Value
Dimension	If we are interested in displaying meshes of a particular dimension, this option may be useful. If there is no mesh with such dimension, the output will be False .	DefaultPrecision
PrintDomain	If Dimension and WorkingPrecision are specified, the corresponding smallest and greatest mesh points will be displayed on screen.	False
PrintMesh	If Dimension and WorkingPrecision are specified, the corresponding mesh will be displayed on screen.	False
WorkingPrecision	It specifies to look for meshes with a given number of digits in accuracy. If only this option and Dimension are specified, the output will be True or False .	DefaultPrecision

corresponding mesh was not previously constructed, **LagMeshEigenvalues** will build it automatically calling **BuildMesh** internally. Therefore, the manual usage of **BuildMesh** can be avoided by the user. After calculations, an ordered list⁸ with the first approximate eigenvalues will be printed on screen. The syntax of the command **LagMeshEigenvalues** is the following:

LagMeshEigenvalues [**V**[**x**], {**x**, **a**, **b**}, **NLevels**, **Dimension**, **Options**]

where

- **V**[**x**] specifies the potential $V(x)$ of the Schrödinger equation (II.8). It must be a numerical expression with one degree of freedom, in this case denoted by **x**.
- {**x**, **a**, **b**} defines the domain in the variable **x** that appears in the potential. The program automatically will select, construct, and map the appropriate mesh for the given domain.

⁸ In ascending order, starting from the lowest eigenvalue.

For a finite interval, semi-finite and infinite, the Legendre, Laguerre, and Hermite are used, respectively.

- **NLevels** represents the number of the lowest eigenvalues that we desire to calculate. Naturally, its value should be a positive integer number.
- **Dimension** defines the size of the mesh, i.e., the number of mesh points.
- There are seven Options that can be set by the user. They are presented in Table III together with a brief description. In addition, all available options of the build-in command **Eigenvalues** are incorporated into **LagMeshEigenvalues**. In general terms, they can be useful to reduce CPU times. Details can be found in the Mathematica® documentation.

There is one important point that we would like to stress. In practical applications, the CPU time and accuracy in approximate eigenvalues are mainly⁹ controlled by three parameters: **Dimension**, **WorkingPrecision**, and **Scaling**. These options make **LagMeshEigenvalues** a versatile command when the user requires fast but highly accurate calculations. Therefore, choosing *appropriate* values for those options is crucial for the performance of the LMM. Explicit examples presented in the next Section will show which considerations must be taken into account when choosing the value of such options.

4. **LagMeshEigenfunctions**

This command delivers as output a list that contains the lowest approximate eigenfunctions of the Schrödinger equation (II.8) defined in (a, b) for a given potential function $V(x)$. By default, they are presented normalized and in the form (IV.1). If the corresponding mesh used for calculations was not previously constructed, **LagMeshEigenfunctions** will build it automatically calling **BuildMesh** internally. Therefore, the manual usage of **BuildMesh** can be avoided by the user. After calculations, an ordered list¹⁰ with the first approximate eigenfunctions will be printed on screen. The syntax of the command is the following:

⁹ The option **Method** will play an important role in applications, see text.

¹⁰ In ascending order, starting from the eigenfunction associated to the lowest eigenvalue.

Table III: Options for (i) **LagMeshEigenvalues**, (ii) **LagMeshEigenfunctions**, and (iii) **LagMeshEigensystem**. Options marked by [†] are only available for commands (ii) and (iii).

Option	Description	Default Value
DiscreteFunction [†]	If it is set to True , the output will be a list that contains a discrete version of the wavefunctions according to (IV.2).	False
ExpectationValue [†]	Function for which the expectation value is calculated via the approximation (II.18).	None
Mass	It fixes the value of the mass (m), see (II.9). Its value must be a positive number.	1
CoefficientsOnly [†]	If it is set to True , the output will be the coefficients c_k that solve the Lagrange equations (II.15).	False
PotentialShift	Shifts the potential $V(x)$ by a real constant. Final results for the spectrum do not depend on the value of this option, see text.	0
Scaling	Its value corresponds to the positive scaling parameter h , defined in (IV.3).	1
WorkingPrecision	It specifies how many digits of precision should be maintained in internal computations. Thus, it controls the numeric accuracy of the approximate spectrum.	MachinePrecision

LagMeshEigenfunctions [**V**[**x**], {**x**, **a**, **b**}, **NLevels**, **Dimension**, **Options**]

The description of each element written above was already presented above when discussing the usage of **LagMeshEigenvalues**. Therefore, the reader is referred to that Section for discussion. The available Options for this command are shown in Table III. In addition, all available options of the built-in command **Eigenvalues** are incorporated into **LagMeshEigenfunctions**.

As a general *heuristic* remark, once we have found *appropriate* values for the options **WorkingPrecision**, **Dimension**, and **Scaling** for **LagMeshEigenvalues**, they are frequently suitable for the command **LagMeshEigenfunctions**. In this way,

the calculation of eigenvalues serves as guidance. As we will see, this argument goes both ways: appropriate values for **LagMeshEigenfunctions** are also appropriate for **LagMeshEigenvalues**.

5. LagMeshEigensystem

This command delivers simultaneously the desired number of eigenvalues and eigenfunctions of the Schrödinger equation (II.8) defined in (a, b) for a given potential function $V(x)$. The syntax is the same as for **LagMeshEigenfunctions**, namely

LagMeshEigensystem[V[x], {x, a, b}, NLevels, Dimension, Options]

In general terms, **LagMeshEigensystem** can be regarded as the combination of the previous two. Therefore, it contains all available options for **LagMeshEigenvalues** and **LagMeshEigenfunctions**, see Table III. In addition, all available options of the built-in command **Eigensystem** are incorporated into **LagMeshEigensystem**.

C. Worked Examples

In this Section, we present different applications of the package for some well-known and relevant systems. The following examples will illustrate and explore how the values of the options can be crucial to obtain accurate eigenvalues and eigenfunctions. A comparison with results from literature is made for some examples. Finally, we encourage the reader to check the supplementary material (**Examples.nb**) to reproduce some of the following calculations. Throughout the rest of this work, unless we specify otherwise, the mass is set to $m = 1$.

1. Exactly Solvable Potentials

We present approximate eigenvalues and eigenfunctions obtained by the **LagrangeMesh** package and compare them with the exact spectrum. We have chosen three potentials that are representative of each possible domain: finite, semi-finite, and infinite. The following examples are helpful to become familiar with the commands and basic options of the package.

a. Particle in a Box. Let us begin with the simplest one-dimensional potential that holds infinitely many bound states: a particle confined to a rigid box of length L . This potential is described by

$$V(x) = \begin{cases} 0, & 0 \leq |x| \leq L \\ \infty, & \text{otherwise} \end{cases} \quad (\text{V.1})$$

The exact solution of the Schrödinger equation leads to the following expression for the eigenvalues

$$E_n = \frac{\pi^2 n^2}{2L^2}, \quad n = 1, 2, \dots, \quad (\text{V.2})$$

On the other hand, using **LagMeshEigenvalues** let us calculate the first 3 lowest eigenvalues using 50 mesh points. To do so, we take $L = 1$ without loss of generality. In this case, the syntax looks like

```
In[3]:= LagMeshEigenvalues[0, {x, 0, 1}, 3, 50, WorkingPrecision->20]
Out[3]:= {4.934802200544679, 19.73920880217872, 44.41321980490211}
```

When comparing with the exact spectrum (V.2), one will note that the error in approximate eigenvalues is of order 10^{-15} . In this case, the error can be reduced (at least) up to 10^{-90} by increasing the value of **WorkingPrecision->200**, but keeping the number of mesh points fixed to $N = 50$. For the present example, we conclude that **WorkingPrecision->20** is insufficient to avoid numerical errors and see the true scope of the LMM.

b. Harmonic Oscillator. This elementary system is described by the potential

$$V(x) = \frac{1}{2}x^2, \quad -\infty < x < \infty. \quad (\text{V.3})$$

remaining eigenvalues are close to the exact ones, but numerical errors are evident. In this case, increasing the value of **WorkingPrecision** is not the solution. However, there are two ways to reduce the errors in this case: (i) increase the dimension of the mesh considering $N > 50$; (ii) choose an appropriate value for **Scaling**. We will postpone the discussion of these two approaches to the following Section.

2. Some Non-Solvable Potentials

In this Section, we consider some representative non-solvable potentials and show how to tackle them with the **LagrangeMesh** package. In what follows, we explore the different options and show how some of them play a fundamental role to obtain highly accurate results for either eigenvalues or eigenfunctions, despite the fact that exact solutions are unknown.

a. Quartic Anharmonic Oscillator. The first example we consider is one of the most studied systems in quantum mechanics: the celebrated quartic anharmonic potential¹³.

$$V(x) = \frac{1}{2}x^2 + \frac{1}{4}x^4, \quad -\infty < x < \infty. \quad (\text{V.8})$$

The discussion is focused on the lowest eigenvalue: the ground state energy denoted by E_0 . In particular, we study the accuracy of the method as a function of the number of mesh points N keeping fixed **WorkingPrecision**→300. As we will see, when considering a sufficiently large value for **WorkingPrecision**, we can ensure that our results are not *contaminated* by a loss of accuracy due to internal arithmetic manipulations. Then convergence of the approximate E_0 will occur as $N \rightarrow \infty$.

We take some representative dimensions from $N = 25$ to $N = 2000$. For the smallest mesh $N = 25$, the block of code looks like

```

In[7]:= LagMeshEigenvalues [  $\frac{1}{2}x^2 + \frac{1}{4}x^4$ , {x, -∞, ∞}, 1, 25, WorkingPrecision→300 ]
Out[7]:= 0.620 927 028 625 317 638 613 539 173 751 . . .
```

We have dropped a considerable number of decimal digits in the output **Out[7]** to sim-

¹³ The present discussion is based on [17].

which is a double well with two degenerate minima located at $x = 0$ and $x = 1/g$. When g is small, it is well-known that there is an exponentially small separation between the energies of the ground (E^-) and first excited (E^+) states [13]. Let us define and denote this energy gap as

$$\Delta E = E^+ - E^- . \quad (\text{V.12})$$

By means of semi-classical analysis [11], we know the first terms of the asymptotic expansion of ΔE , namely

$$\Delta E_{SC} = -\frac{2}{\sqrt{\pi g}} e^{-\frac{1}{6g^2}} \left(1 - \frac{71}{12} g^2 + \mathcal{O}(g^2) \right) + \mathcal{O} \left(e^{-\frac{1}{3g^2}} \right) , \quad (\text{V.13})$$

where the sub-index SC stands for semi-classical. Let us investigate if the LMM can capture the exponentially small contribution in the energy gap for $g = 1/30$. Let us point out that the degenerate minima are $x = 0$ and $x = 30$. Therefore, the mesh that we need to consider must cover these two points. It turns out that $N = 1000$ is appropriate, as shown in the following input where we print on screen the smaller and largest mesh points, see `In[8]` and `Out[8]`.

```
In[8]:= AvailableMeshQ["Hermite", Dimension->1000, WorkingPrecision->300,
PrintMesh->True]
Out[8]:= {-44.2092, 44.2092}
```

Now we calculate the first two eigenvalues using the Hermite mesh, see `In[9]` below.

```
In[9]:= g = 1/30;
LagMeshEigenvalues[1/2 x^2 (1-g x)^2, {x, -∞, ∞}, 2, 1000, WorkingPrecision->300,
Method->"Arnoldi"]
Out[9]:= {0.498883271316609786728219605658571743939794419539193419407486112020...,
0.498883271316609786728219605658571743939794419539193419407486112262...}
```

We have introduced the built-in option `Method->"Arnoldi"` to reduce CPU times: from 1.2 hrs to 5 min. In addition, the last digits of the output were removed. From the two first eigenvalues, we can estimate the energy gap and compare with (V.13):

$$\Delta E_{LMM} = 2.4129 \times 10^{-64} , \quad \Delta E_{SC} = 2.4128 \times 10^{-64} . \quad (\text{V.14})$$

We can see that there is an excellent agreement between both estimates¹⁵. Let us now investigate how the wavefunctions look like with respect to x . Since the dimension of the basis is quite large ($N = 1000$), it is convenient to use the discrete version of the wavefunction to avoid loss of accuracy. To do so, we use input `In[10]` shown below.

```
In[10]:= g = 1/30;
LDW = LagMeshEigenfunctions[1/2 x^2 (1 - g x)^2, {x, -∞, ∞}, 2, 1000,
WorkingPrecision -> 300, Method -> "Arnoldi", DiscreteFunction -> True];
```

In the previous block of code, we have stored the discretized wavefunctions in a list called `LDW`. Then, the plots of the first two wavefunctions can be easily obtained using the built-in command `ListPlot`,

```
In[11]:= ListPlot[LDW[[1]], PlotRange -> All, Joined -> True]
```

The output of the previous block `In[11]` corresponds to the plot of the ground state eigenfunction shown in Fig. 2. With minimal modifications, the same block can be used to plot the first excited wavefunction, see Fig. 3.

There is one point that should be emphasized about the Hermite mesh used in this example. By construction, it always will be symmetrical with respect to the vertical axis ($x = 0$). As a consequence, the discrete version of the wavefunction will be defined for mesh points inside $-x_N \leq x \leq x_N$. However, it can be seen from Figs. 2 and 3 that the wavefunction do not share the same symmetry of the domain. Furthermore, wavefunctions are negligibly for $x < -10$. To improve the performance of the LMM, it is natural to shift/translate the potential $V(x) \rightarrow V(x + 1/2g)$ to make it symmetrical under $x \rightarrow -x$. Naturally, final results for the spectrum do not depend on the shift. For instance, $N = 500$ can provide the same accuracy for the energy gap in comparison with previous calculations with $N = 1000$. In this case, CPU time was reduced from 20 min to 50 s.

c. Shell-Confined Hydrogen Atom. This system is described by the Schrödinger equation (II.8) with the usual Coulomb potential $V(r) = -1/r$. The difference comes from the

¹⁵ SC-estimate was calculated neglecting terms of $\mathcal{O}(g^2)$ and $\mathcal{O}(e^{-1/3g^2})$ in (V.13)

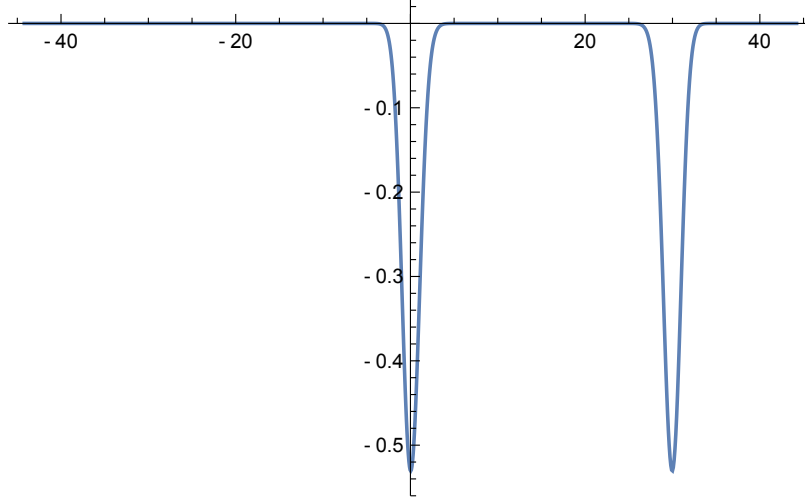


Figure 2: Approximate wavefunction of the ground state in the double-well potential (V.11). Plot generated by `ln[10]` and `ln[11]`.

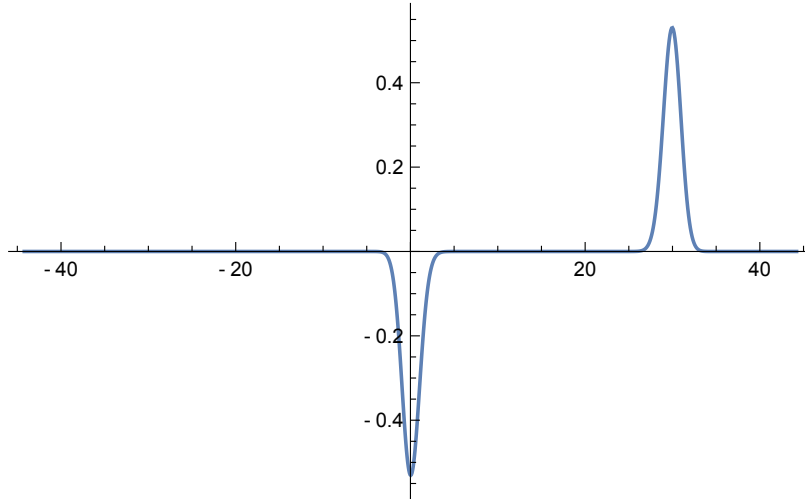


Figure 3: Approximate wavefunction of the first excited state in the double-well potential (V.11). Plot generated via `ln[10]` and minimal modifications of `ln[11]`.

boundary conditions which guarantee the shell-type configuration:

$$\psi(r_1) = \psi(r_2) = 0, \quad 0 \leq r_1 < r_2. \quad (\text{V.15})$$

Let us take as an example the particular core-shell configuration

$$r_1 = 10, \quad r_2 = 100, \quad (\text{V.16})$$

and calculate the first three energies for angular momentum $\ell = 2$. To do so, we use `ln[12]`. In this way, we confirmed the results provided in Ref. [18]. However, further calculations

```

In[12]:= l = 2;
LagMeshEigenvalues[- $\frac{1}{r} + \frac{1(1+1)}{2r^2}$ , {r, 12, 100}, 3, 100, WorkingPrecision→30,
PotentialShift→1]
Out[12]:= {-0.0312499999998759365128795, -0.0191184570787652150378327,
-0.0131200561664748472136198}

```

can easily overcome those benchmarks by increasing the number of mesh points and using higher `WorkingPrecision`. We note that the first eigenvalue in the list is very similar to the energy of the familiar states¹⁶ of the *free* hydrogen atom with principal quantum number $n = 4$, which is $E_4 = -1/32$. This is not a coincidence, the usual wavefunction for the state $4d$ has a node at $r_1 = 12$ and another one at $r_2 = \infty$. In this example $r_2 = 100$ is sufficient to mimic " ∞ ". This phenomenon will be explained below.

d. \mathcal{PT} -symmetric cubic oscillator For some systems defined on a semi-finite or infinite interval, it is enough to confine them in a sufficiently large box. We explore such situation based on a particular example. Let us take,

$$V(x) = ix^3, \quad -\infty < x < \infty. \quad (\text{V.17})$$

This potential is invariant under the simultaneous transformations¹⁷ $x \rightarrow -x$ and $i \rightarrow -i$ as well as the kinetic term in the Hamiltonian. It is well-known that the spectrum associated with this potential is positive and discrete [19]. Using the package, we can easily obtain the first eigenvalues with unprecedented accuracy. For this purpose, we use the following block of code.

```

In[13]:= LagMeshEigenvalues[I x3, {x, -∞, ∞}, 5, 200, WorkingPrecision→100]
Out[13]:= {0.76285177422726354... + 1.82697736694870898... × 10-113 I,
2.71107992325388461... + 8.06725746334795611... × 10-106 I,
4.98924008753779726... + 7.36353994216817421... × 10-103 I,
7.46473454878490666... + 1.50123757767888490... × 10-73 I,
10.0886630708259331... + 1.69712257011508907... × 10-47 I}

```

Eigenvalues in `ln[13]`. are essentially real, with a small imaginary part. In particular,

¹⁶ Associated with the potential (V.5).

¹⁷ \mathcal{PT} -symmetry stands for \mathcal{P} arity and \mathcal{T} ime reversal.

the first three are consistent with the requested accuracy of 100 exact digits in arithmetic. Since the potential (V.17) is defined in the whole real line, it was natural to specify the domain $\{\mathbf{x}, -\infty, \infty\}$ inside **LagMeshEigenvalues**. However, with a sufficiently large finite domain¹⁸, it is possible to reproduce exactly those results as shown below.

```
In[14]:= LagMeshEigenvalues[I x^3, {x, -10, 10}, 5, 200, WorkingPrecision->100]
Out[14]:= {0.76285177422726354... + 6.60062084477509384... x 10^-108 I,
           2.71107992325388461... + 1.53860672832849900... x 10^-100 I,
           4.98924008753779726... + 1.28045707882104121... x 10^-96 I,
           7.46473454878490666... + 2.47157825497472030... x 10^-75 I,
           10.0886630708259331... + 1.40906101716468556... x 10^-47 I}
```

The real part of numerical eigenvalues in **Out[14]** is confirmed, meanwhile the imaginary part is different but still small. Previous results obtained by the LMM overcome benchmarks found in literature, see [19].

e. Quasi-Exactly Solvable Double Well. From [20], we extract the one-dimensional potential¹⁹:

$$V(x) = x^6 + 2x^4 - 18x^2 - 1, \quad \infty < x < \infty. \quad (\text{V.18})$$

Degenerate minima are located approximately at $x = \pm 1.368$. For this potential, only the five lowest eigenfunctions²⁰ of even parity can be found in exact form. They can be written as

$$\psi_n(x) = P_n(x^2)e^{-\frac{1}{2}x^2 - \frac{1}{4}x^4}, \quad n = 0, 1, \dots, 4, \quad (\text{V.19})$$

where $P_n(x)$ is a real polynomial of degree n . Correspondingly, eigenvalues and eigenfunctions can be computed via simple algebra. In particular, eigenvalues read

$$\begin{aligned} E_0 &= -14.044\,499\,331, & E_1 &= 3.247\,407\,444, & E_2 &= 4.623\,648\,530, \\ E_3 &= 17.853\,104\,881, & E_4 &= 34.815\,153\,363. \end{aligned} \quad (\text{V.20})$$

In this example, we now study the effect of **Scaling** on the accuracy of the method keeping the number of mesh points fixed ($N = 30$). First, Let us calculate the first nine eigenvalues using **LagMeshEigenvalues**, and then extract those which correspond to even parity.

¹⁸ A similar phenomenon occurred in the previous Section for the shell-confined hydrogen atom.

¹⁹ In [20], equation (2.1), $a = b = 1$, $k = 0$, and $n = 4$.

²⁰ In the Hamiltonian operator (II.9) the mass must be taken as $m = 1/2$.

The input `In[15]`, shown below, works for this purpose.

```
In[15]:= LagMeshEigenvalues [  $\mathbf{x}^6 + 2\mathbf{x}^4 - 18\mathbf{x}^2 - 1$ , { $\mathbf{x}$ ,  $-\infty$ ,  $\infty$ }, 9, 30, WorkingPrecision→20,
Mass→1/2]
Out[15]:= { -14.08077227171645238, ..., -3.2475575741665341, ..., 4.8786311954474445,
..., 18.5854712028856120, ..., 29.1878679181253049 }
```

Since we are interested in even parity states, we have replaced the energies of odd states with dots in the output `Out[15]`. Compared with (V.20), we note that numerical results are not very accurate, especially for excited states. The performance of the method can be improved if we choose an adequate scaling parameter. For this purpose, it is sufficient to calculate and plot the discrete version of the ground state wavefunction. For this purpose we use `In[16]`. The corresponding output is the plot is presented in Fig. 4. From this plot,

```
In[16]:= LGS = LagMeshEigenfunctions [  $\mathbf{x}^6 + 2\mathbf{x}^4 - 18\mathbf{x}^2 - 1$ , { $\mathbf{x}$ ,  $-\infty$ ,  $\infty$ }, 1, 30, Mass→1/2,
WorkingPrecision→20, DiscreteFunction→True];
ListPlot [ LGS, Joined→True, Mesh→All]
```

we note that the wavefunction is small ($\sim 10^{-4}$) for $|x| \geq 3.5$. Therefore, it is convenient to scale the mesh to move all mesh points to the region $|x| \leq 3.5$, where the function is not too small. This can be done by means of **Scaling**. For this particular case, **Scaling** $\rightarrow 1/2$ seems to be suitable. Recalculating the spectrum with this scaling, we obtain more accurate approximate energies, especially for excited states. This can be check in the block of code for `In[17]`.

f. Rydberg Atoms. As final example, we show how **LagMeshEigensystem** works. Let us consider the following radial potential

$$V(r) = -\frac{Z_\ell(r)}{r} - \frac{a_c}{2r^4} \left[1 - e^{-(r/r_c)^6} \right] + \frac{\ell(\ell+1)}{2r^2} \quad (\text{V.21})$$

where

$$Z_\ell(r) = 1 + (Z - 1)e^{-a_1 r} - r(a_3 + a_4 r)e^{-a_2 r} \quad (\text{V.22})$$

where $\{a_1, a_2, a_3, a_4, r_c, a_c\}$ are parameters with dependence on the value of ℓ (angular momentum) and the atomic number Z . Potential (V.21), written in a.u, is useful to study the so-called Rydberg atoms. It describes a highly excited electron of valence through a radial potential [21]. The spin-orbit interaction has been dropped for simplicity. For concreteness,

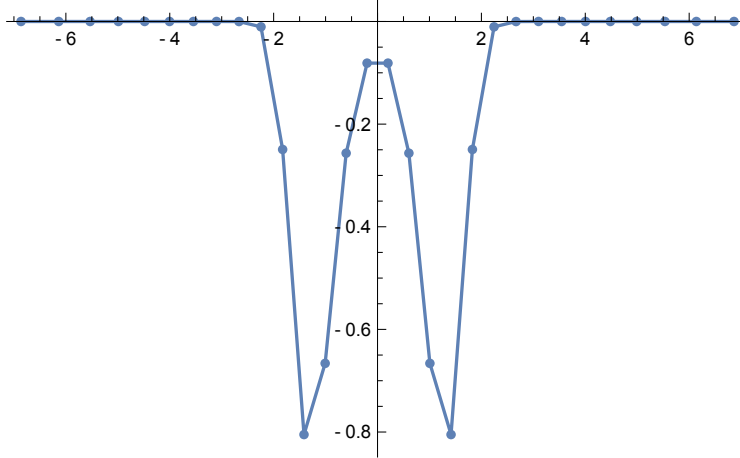


Figure 4: Approximate discrete ground state wavefunction of the quasi-exactly solvable potential (V.18). For $N = 30$, mesh points are distributed in the domain $-7 < x < 7$. Plot generated via `In[16]`.

```
In[17]:= LagMeshEigenvalues[ $x^6 + 2x^4 - 18x^2 - 1$ , { $x$ ,  $-\infty$ ,  $\infty$ }, 9, 30, WorkingPrecision $\rightarrow$ 20,
  Mass $\rightarrow$ 1/2, Scaling $\rightarrow$ 1/2]
Out[17]:= {-14.04449918094238512, ..., -3.2474090114716549, ..., 4.6236364005060602,
  ..., 17.8529954304045896, ..., 34.8150945730654724}
```

we focus on the p -states associated to the valence electron of the Rubidium (Rb) atom, thus, we take $Z = 37$ and $\ell = 1$. The values of the parameters in a.u. that characterize (V.21) and (V.22) are the following²¹

$$\begin{aligned}
 a_c &= 9.0760, & r_c &= 1.50195124, \\
 a_1 &= 4.44088978, & a_2 &= 1.92828831, & a_3 &= -16.79597770, & a_4 &= -0.81633314.
 \end{aligned}
 \tag{V.23}$$

To calculate eigenvalues and eigenfunctions simultaneously, we use the block of code shown below, see `In[18]`.

A Laguerre mesh with $N = 20$ is more than sufficient to obtain the first two eigenvalues and eigenfunctions with accuracy consistent with the number of digits in the parameters (V.23). In the previous calculation, **Scaling** is crucial to obtain a good performance of the command **LagMeshEigensystem** as we now explain. First, note that the potential

²¹ See reference [21].

```

In[18]:= l = 1;
         z = 37;
         tol = 10-20;
         ac = Rationalize[9.0760, tol];
         rc = Rationalize[1.50195124, tol];
         a1 = Rationalize[4.44088978, tol];
         a2 = Rationalize[1.92828831, tol];
         a3 = Rationalize[-16.79597770, tol];
         a4 = Rationalize[-0.8163314, tol];
         Z1[r_] := 1 + (z-1) Exp[-a1 r] - r (a3 + a4 r) Exp[-a2 r];
         V[r_] := - $\frac{Z1[r]}{r}$  -  $\frac{ac}{2r^4} (1 - \text{Exp}[-(r/rc)^6]) + \frac{1(1+1)}{2r^2}$ ;
         LagMeshEigensystem[V[r], {r, 0,  $\infty$ }, 2, 20, WorkingPrecision $\rightarrow$ 20,
           Scaling $\rightarrow$ 1/30]
Out[18]:= {{-64.333486..., 2 $\times$ 51/2 Exp[-10r] (-3.960999... $\times$ 10-6 r + ...)},
          {-6.307591..., 2 $\times$ 51/2 Exp[-10r] (-7.242503... $\times$ 10-7 r + ...)}}

```

(V.21) develops a deep well (depth ~ -216 a.u.) of small width ~ 0.5 a.u. Therefore, the wave function is localized in a very small spatial region. Via **Scaling** we can move all mesh points to such region. This increases the accuracy in results and reduces CPU times from minutes to a couple of seconds.

Before concluding, there is a technical issue that should be mentioned concerning potential (V.21). Since exponential functions are involved, the evaluation of potential matrix elements (II.16) can lead to extremely small numbers. This might lead to a loss of accuracy in calculations and to an increment in CPU times. This situation has to be avoided as much as possible. For the particular previous case, **Scaling \rightarrow 1/30** solves the situation. Usually, if the energy calculated by using a given mesh is accurate, the corresponding eigenfunctions will be as well. The reader is referred to the supplementary material to check this statement for the two lowest states of the Rydberg atom considered above.

3. Possible Issues

We give a brief review of common situations that the user may face.

a. Loss of Accuracy. In order to use arbitrary precision arithmetic offered by Mathematica[®], specified basically by the option **WorkingPrecision**, it is mandatory to define all input parameters (**V[x]**, **Dimension**, **Mass**, **Scaling**, *etc.*) with the same accuracy chosen for

WorkingPrecision. In general, defining all of them with absolute accuracy is more than enough. For example, instead of taking **1.5**, use **3/2**. Otherwise, accuracy in arithmetic will drop to **MachinePrecision**. Avoiding extremely small/large numbers can help the performance as well. For example, considering **Mass**→**9.1093837015**×**10**⁻³¹ (kg), which is the mass of the electron, will lead to a poor performance of the method. Therefore, it is advisable to use the natural scales of the system.

Another situation that leads to a limited accuracy in the spectrum occurs when the wavefunctions are very extended in the domain. This is typical for weakly bound states defined on semi-infinite²² or infinite domains.

b. CPU times and RAM. Computation time may become significant in different situations. Usually, either large values of **Dimension** or **WorkingPrecision** require more CPU time. In particular, constructing accurate and large meshes via **BuildMesh** can take days of calculations. Choosing an appropriate value of **Scaling**, instead of increasing the size of the mesh, can lead not only to an improvement of results, but also to a reduction of CPU times. When few eigenvalues or eigenfunctions are of interest, the option **Method**→"**Arnoldi**" usually reduces CPU times drastically. Let us point out that an increase in **WorkingPrecision** will certainly increase the arithmetic accuracy. However, the RAM needed to manipulate and store those numbers during calculations will become larger. It is highly recommendable to keep track of RAM consume from the terminal.

c. Limitations. Any approximate method to solve the Schrödinger-type equations has its own *domain of applicability*. The LMM is not the exception. One limitation comes from the Gauss quadrature approximation. When the potential is not smooth, the Gauss quadrature fails and, as a result, matrix elements $V_{i,j}^{(G)}$ may be inaccurate. Certainly, this will lead to a poor accuracy in the spectrum. A simple representative example of this situation occurs for the one-dimensional potential

$$V(x) = |x|, \quad -\infty < x < \infty, \quad (\text{V.24})$$

which is not smooth at $x = 0$. Using **LagMeshEigenvalues**, even with a large number of mesh points, eigenvalues are inaccurate, see [In\[19\]](#) and [Out\[19\]](#).

²² The usage of the LMM in this situation has already been investigated in [22].

```
In[19]:= LagMeshEigenvalues [ Abs [ x ] , { x , -∞ , ∞ } , 1 , 1000 , WorkingPrecision → 300 ]
Out[19]:= 0.808632...
```

If we compare it with the *exact* lowest eigenvalue $E_0 = 0.808616\dots$, we can immediately note the poor performance of the **LagrangeMesh** package.

VI. CONCLUSIONS

Through the years, many efforts have been put into developing numerical methods to solve the time-independent one-dimensional Schrödinger equation. In this work, we focused on one of these methods to study bound states: the Lagrange Mesh method (LMM). Specifically, the LMM is an approximate variational method simplified by a Gauss quadrature associated with a given mesh. The method is based on three ingredients: Gauss quadrature approximation, Lagrange functions, and secular equations. The non-existent ideal numerical method would be characterized by (i) short CPU times; (ii) high accuracy; (iii) applicable to any potential. Under some conditions, the LMM fulfills these three characteristics.

After presenting a comprehensive and detailed discussion of the LMM, we introduced the **LagrangeMesh** Mathematica[®] package. It provides the user three commands that implement the LMM numerically: **LagMeshEigenvalues**, **LagMeshEigenfunctions**, and **LagMeshEigensystem**. The output of each one is the following: eigenvalues, eigenfunctions, and eigenvalues and eigenfunctions, respectively. All of them are delivered on screen in such a way that they are ready-to-use. Therefore, we have a powerful tool to find the quantum spectrum of an arbitrary potential defined on a given interval (which can be finite, semi-finite, or infinite). Two complementary commands, **BuildMesh** and **AvailableMeshQ**, are available to the user to construct and check meshes and weights. All five commands are user-friendly and none of them requires more than a couple of lines to specify the input. The main properties of the commands offered by the package are (i) efficiency; (ii) control of the accuracy in arithmetic manipulations and final results. These properties are controlled by three options **Dimension**, **Scaling**, and **WorkingPrecision**.

Based on different relevant physical systems (*worked examples*), we discussed in detail

the usage, scope, and limitations of the package. In particular, for some of those systems, we showed explicitly how benchmarks in eigenvalues are established in few lines of code in short CPU times. For example, we established the most accurate results for the first energies of the \mathcal{PT} -symmetric cubic potential. The collection of worked examples presented in the text can be regarded as a user guide of the package.

Finally, the **LagrangeMesh** package may serve as a tool for educational and research purposes. In particular, it can be used to test other highly accurate methods of different nature.

ACKNOWLEDGMENTS

I am very grateful to H. Olivares-Pilón for the outstanding and comprehensive lectures about the LMM. I thank A.V. Turbiner for the constant encouragement in developing the package, many useful discussions, comments, and suggestions. I thank S. Cárdenas-López for useful remarks and tests of the package. Finally, I would like to thank K. Kropielnicka for valuable suggestions and careful reading of the text. This work is partially supported by the Simons Foundation Award No. 663281 granted to the Institute of Mathematics of the Polish Academy of Sciences for the years 2021-2023. Additional financial support was provided by the SONATA BIS-10 grant no. 2019/34/E/ST1/00390.

-
- [1] E. Schrödinger, *Ann. Phys.* **385**, 437 (1926).
 - [2] D. Baye, *Phys. Rep.* **565**, 1 (2015).
 - [3] M. Hesse and D. Baye, *J. Phys. B* **32**, 5605 (1999).
 - [4] M. Hesse and D. Baye, *J. Phys. B* **37**, 3937 (2004).
 - [5] H. Olivares Pilón and D. Baye, *Phys. Rev. A* **88**, 032502 (2013).
 - [6] Z. Wang, Y. Ge, Y. Dai, and D. Zhao, *Comput. Phys. Commun.* **160**, 23 (2004).
 - [7] T. Sulejmanpasic and M. Ünsal, *Comput. Phys. Commun.* **228**, 273 (2018).
 - [8] G. D. Xavier, *Comput. Phys. Commun.* **278**, 108419 (2022).
 - [9] R. M. Fonseca, *Comput. Phys. Commun.* **267**, 108085 (2021).

- [10] P. H. Jacobse, *Computer Physics Communications* **244**, 392 (2019).
- [11] J. Zinn-Justin and U. D. Jentschura, *Ann. Phys.* **313**, 197 (2004).
- [12] K. E. Atkinson, *An introduction to numerical analysis* (John wiley & sons, 2008).
- [13] L. D. Landau and L. M. Lifshitz, *Quantum Mechanics Non-Relativistic Theory, Third Edition: Volume 3*, 3rd ed. (Butterworth-Heinem, 1981).
- [14] J. D. Castaño-Yepes, O. Franca, C. Ramirez-Gutierrez, and J. C. del Valle, *Phys. E: Low-Dimens. Syst. Nanostructures* **123**, 114202 (2020).
- [15] Wolfram Support Quick Answers, “<https://support.wolfram.com/5648?src=mathematica>”.
- [16] J. J. Sakurai, *Modern quantum mechanics; rev. ed.* (Addison-Wesley, Reading, MA, 1994).
- [17] A. V. Turbiner and J. C. del Valle, *Int. J. Quantum Chem.* **121**, e26766 (2021).
- [18] K. D. Sen, *J. Chem. Phys.* **122**, 194324 (2005).
- [19] C. M. Bender and S. Boettcher, *Phys. Rev. Lett.* **80**, 5243 (1998).
- [20] A. V. Turbiner, *Phys. Rep.* **642**, 1 (2016).
- [21] M. Marinescu, H. R. Sadeghpour, and A. Dalgarno, *Phys. Rev. A* **49**, 982 (1994).
- [22] J. C. del Valle and D. J. Nader, *J. Math. Phys.* **59**, 102103 (2018).